

# Stalling in Space: Attractor Analysis for any Algorithm

Sarah L. Thomson<sup>1</sup>, Quentin Renau<sup>1</sup>, Diederick Vermetten<sup>2</sup>, Emma Hart<sup>1</sup>, Niki van Stein<sup>2</sup>, and Anna V. Kononova<sup>2</sup>

2

**Abstract.** Network-based representations of fitness landscapes have grown in popularity in the past decade; this is probably because of growing interest in *explainability* for optimisation algorithms. Local optima networks (LONs) have been especially dominant in the literature and capture an approximation of local optima and their connectivity in the landscape. However, thus far, LONs have been constructed according to a strict definition of what a local optimum is: the result of local search. Many evolutionary approaches do not include this, however. Popular algorithms such as CMA-ES have therefore never been subject to LON analysis. Search trajectory networks (STNs) offer a possible alternative: nodes can be any search space location. However, STNs are not typically modelled in such a way that models temporal *stalls*: that is, a region in the search space where an algorithm fails to find a better solution over a defined period of time. In this work, we approach this by systematically analysing a special case of STN which we name *attractor networks*. These offer a coarse-grained view of algorithm behaviour with a singular focus on stall locations. We construct attractor networks for CMA-ES, differential evolution, and random search for 24 noiseless black-box optimisation benchmark problems. The properties of attractor networks are systematically explored. They are also visualised and compared to traditional LONs and STN models. We find that attractor networks facilitate insights into algorithm behaviour which other models cannot, and we advocate for the consideration of attractor analysis even for algorithms which do not include local search.

**Keywords:** fitness landscape, local optima networks, search trajectory networks

## 1 Introduction

Understanding the landscape or structure of the search space associated with a problem instance is important for both predicting the performance of algorithms and improving algorithm design so that they can more efficiently traverse the landscape. In the past decade, several techniques for visualising landscapes have arisen that provide new insights into this task. Local optima networks (LONs) [1] capture the number, distribution and connectivity pattern of local optima in the form of a network where nodes represent local optima and edges capture the

transitions between them. LONs have most often been used to understand landscapes in combinatorial settings [2,3,4] — mainly due to the fact that constructing a LON requires an iterated local search (ILS) algorithm to be run to identify local optima. More recently, LONs have been constructed for continuous spaces, mostly using monotonic basin-hopping [5,6], which is essentially an ILS framework for continuous optimisation. The LON model has been particularly useful identifying basins of attraction in a landscape [4,7]. Search trajectory networks (STNs) [8] were introduced as a more generalisable alternative to LONs. STNs are directly constructed from data gathered while running an algorithm. Unlike LONs, there is no condition that nodes must be a local optima. STNs enable a user to visualise (for example) whether multiple algorithms or runs of an algorithm traverse the same locations, indicate termination points of an algorithm (both optimal and sub-optimal) and show the frequency with which algorithms pass through and escape from the nodes via an edge weight. However, STNs do not typically provide information as to **how long** an algorithm remained stalled at a node before managing to escape — the information they encode is valuable, but does not generally have this temporal aspect.

To address this, we put forward a new variant of an STN which is applicable to any type of algorithm (including those that do not easily permit local search) and which demonstrate the *stagnation behaviour* of an algorithm at various points in the search. We dub these regions *stall locations*: a period of the search process where the best value of the objective function does not change over a period of  $\beta$  evaluations. A stall location can hence be seen as an attractor of the search and can be detected using any type of algorithm (i.e. it does not rely on local search). This approach, which we call *attractor networks*, brings new insights into the operation of algorithms which are not evident in either LON networks or STN networks. We study the properties and illustrate the benefits of attractor networks by constructing them using three different algorithms on the 24 functions of the BBOB test suite [9] — comparing metrics and visualisations obtained from the networks to those obtained from both LON and STN. The contributions can be summarised as follows:

- The formal introduction of a method for visualising and analysing attractors in the genotype space (termed an *attractor network, or AN*) in a landscape that is applicable to algorithms from both the continuous and combinatorial optimisation domains and regardless of whether local search is applicable.
- A demonstration that ANs can provide new insights into intermediate attractors in the search process that are not detected by standard LON or STN analysis, obtained by evidence gathered by conducting a systematic analysis over suite of functions and algorithms.

## 2 Background

### 2.1 Network models

*Local optima network (LON)*. A local optima network is a directed and weighted graph comprised of: a) nodes  $lo_i \in LO$  which belong to a set of local optima (this

can be the complete set or a sample) and b) edges  $e_{ij} \in E$  which connect pairs of local optima (nodes)  $lo_i$  and  $lo_j$  with a weight which denotes the frequency of transition  $w_{ij}$  iff  $w_{ij} > 0$ . Extensive descriptions can be found in [10].

*Search trajectory network (STN).* A search trajectory network is a directed and weighted graph comprised of: a) nodes  $sl_i \in SL$  which belong to a set of search locations from algorithm trajectories (these do not need to be local optima) and b) edges  $e_{ij} \in E$  which connect pairs of locations (nodes)  $sl_i$  and  $sl_j$  with a weight which denotes the frequency of transition  $w_{ij}$  iff  $w_{ij} > 0$ . Extensive descriptions can be found in [11].

## 2.2 LON and STN manifestations

In combinatorial spaces, LONs are constructed such that a local optimum is the result of the application of a local search method [10]. In this way, the LON nodes satisfy the condition that they are the best solution within their [sampled or complete] neighbourhood with respect to a basic mutation operator. This is usually achieved either by using iterated local search as the construction algorithm [2,3,4] or occasionally by augmenting population-based approaches with local search, rendering them memetic [12,13].

Approaches in continuous spaces are typically similar; the Limited-memory Boyden-Goldfarb-Shanno (L-BFGS-B) [14] optimiser — a quasi-Newton method — has been used as local search to obtain LON nodes [5,6,15]. The Nelder-Mead downhill simplex algorithm has been used as an alternative method to identify local optima for LONs [16]; very recently, a greedy local sampling akin to  $(1 + \lambda)$  Evolutionary Strategy has been proposed for discovering local optima for these purposes [17]. One contribution augmented differential evolution with local search so that LONs could be constructed [18]. The common thread with LON works in continuous spaces is that the network is constructed using algorithms which may not always closely resemble the type of algorithms actually used to search these kind of spaces in practice. For example, networks which reflect the dynamics encountered by monotonic basin-hopping may only give *limited insight* into how CMA-ES behaves on a problem.

STNs are more generalisable than LONs, but have their own considerations. One is the decision of when to log a new STN node. As it relates to population-based algorithms moving in continuous spaces, the convention is logging the best individual in the population every  $G$  generations;  $G$  has been set as (for example) 1 [11] or the dimension of the problem [8]. This could potentially have the effect that a location is logged even if the search is only there for as little as one generation.

Very recently, an article on Cartesian genetic programming (CGP) [19] took the alternative approach of logging STN nodes if the search was at a location in the behaviour space for at least one iteration. However, in practice, the search was usually stuck at locations in the behaviour space for many iterations. It is therefore the case that what resulted was essentially an attractor network (as it is defined in this paper), although there are some *key differences*: a) this was

not in the genotype space, as we consider here; b) a single node in the behaviour network represented typically thousands of genotypically different solutions from the genotype space which map to the same program behaviour; and c) the condition for a behaviour location to be considered a stall point was a single iteration. Despite the differences with the networks we analyse here, in that work attractors were visualised and this helped give valuable comparative insights about the two studied CGP algorithms. This finding serves as a good motivator for our work in focussing on attractors.

Another choice related to STN modelling in continuous spaces is what the threshold in decision space should be defined to consider two solutions the same. For this, a *partition factor* has been used [8,11]. The same concept has also been used in LON analysis for continuous functions; the original paper used a threshold of  $10^{-5}$  [5] and this is also the value used in the Python package PFLACCO [20]. With STNs, the partition factor has conventionally been decided according to a formula involving the search space bounds,  $x_{max}$  and  $x_{min}$  and dimension of the problem. They consider the largest integer  $n$  for which the following holds:  $(x_{max} - x_{min}) \times D \geq 10^n$ ; with  $n$ , the expression  $2 - n$  is then carried out to obtain the partition factor, which is equivalent to the exponent of 10. According to this formula, our partition factors would lead to coordinate precision  $\epsilon = 10^{-1}$  for 2D and  $\epsilon = 10^0$  for 10D. This is rather coarse when we consider that our region of interest is  $[-5, 5]$ ; we therefore take  $10^{-2}$  as our most coarse setting, but also consider other lower values which are specified in Section 4.

It is standard with visualisation of STNs to make the size of the nodes proportional to how many search runs reached that location [21] and the related notion of *attraction areas* has been considered recently [22]; however, these ideas are *not* equivalent to the notion of attractor which we use in this paper. The visual node sizes and identified attraction areas will show locations where search goes frequently, **but not how long it stays there**. For example: a node which is large in a standard STN visualisation could represent a location where search flows through often, but where it does not stay for longer than a single generation of the algorithm. There could also be a case where a node is small — due to having only been found in a single run — but search stalled there for a significant number of evaluations before finally moving on. This would not be captured with standard STN conventions, but is important to capture. In general, neither LONs nor STNs typically consider the temporal aspect of algorithm behaviour directly. That thought, alongside an appetite for applying LON analysis to real-world problems (where the relevant search algorithms may not mirror LON construction methods, but attractors may nevertheless be of great importance), motivates the idea of attractor networks introduced here.

### 2.3 The Notion of Attractors for CMA-ES and DE

As introduced in Section 4, experiments carried out in this study are based on variants of two popular heuristic algorithms for continuous setting: CMA-ES and

DE. Therefore, we briefly examine the literature for the analysis of attractors and these two algorithm classes.

To the best of our efforts, no papers were identified that consider search behaviour in the sense of stalling moments or locations during runs of continuous optimizers. While not really discussing the concept of stalling/attractors per se, the heuristic (continuous) optimisation community has actively worked on mechanisms preventing such stalling. These include: restarts of stagnated [23] or redundant [24] runs with possible increase of population size (IPOP [23] and BIPOP [25] mechanisms in CMA-ES and adaptive population control [26,27] in DE), step-size thresholding [28] and control of covariance matrix eigenvalues in CMA-ES, various population diversity improving components for both algorithms, improved covariance adaptation mechanisms for high-conditioned landscapes, improved handling of boundary constraints to balance exploration of the whole domain [29].

### 3 Methodology

#### 3.1 Attractor Networks

In the context of optimisation algorithms, the notion of attractors can be defined in a traditional sense inspired by [30,31] that is independent of the algorithm, as described in [32]. For a metric space  $X$ , the basin of attraction in discrete-time dynamics is defined for the system  $(X, \varphi : X \rightarrow X)$ , where the  $k$ -th iteration of the system corresponds to the  $k$ -fold composition  $\varphi \circ \varphi \circ \dots \circ \varphi(\cdot)$ . The application of  $\varphi$  to  $x$  is assumed to shift  $x$  towards a vector of smaller magnitude in the direction opposite to  $\nabla f(x)$ . If this iterative process converges to a single point  $x$  such that  $\varphi(x) = x$ , this point is referred to as an *attractor*.

*Attractor.* In the context of attractor networks, we define an *attractor* to be a location in the search space where at least one of the  $r$  algorithm runs used to construct the network stalled for at least  $\beta$  fitness evaluations. We are working in continuous spaces in this study; it follows that the notion of attractor also depends on the coordinate precision  $\epsilon$ . This value mandates the cutoff threshold in decision space for two solutions to be considered the same attractor node in the network: if the two solutions differ in at least one variable by an amount equal to or over  $\epsilon$  then they will not be represented by the same node.

*Attractor network construction.* Attractor networks can be constructed from a log taken during algorithm runs. The log must include all moments of improvement to the best-so-far solution; each logging event will consist of three things: the number of elapsed fitness evaluations, the fitness of the new solution, and the genotype of that solution. From this type of log, an attractor network can be built in mostly the same manner as an STN, except nodes (and edges) are **exclusively** logged if the number of elapsed evaluations between two consecutive improvements to the best-so-far solution is greater than  $\beta$ . Mirroring LONs and

STNs, an attractor network is comprised of the trajectories for multiple independent runs of the algorithm. The network is also defined according to a level of coordinate precision  $\epsilon$ : the radius in decision space [computed with Manhattan distance] within which two solutions are considered the same node.

*A note on attractor networks.* We note that standard LONs are a special case of STNs, essentially encoding search trajectories of monotonic basin-hopping (in continuous space) or iterated local search (combinatorial). The attractor networks described here may be seen as both LONs and STNs — although, instead of strict hill climbing local optima we consider generalised attractors. The perspective is non-specific enough that any algorithm can be studied using it, unlike LONs. STNs can also be used to understand any algorithm, but they have not been modelled in such a way that attractor structure in the genotype space is evident. Attractor networks could be viewed as a reduced STN, and essentially offer a coarser-grained view with a singular focus on search traps.

### 3.2 Approach to validation

Naturally, the attractor networks should be compared with standard local optima networks and standard search trajectory networks. This brings to mind the question of what ‘standard’ means for these models; we now clearly define what we consider to be the standard models (for the purposes of the study). We define the standard LON as the method implemented in PFLACCO and described fully in previous literature [5]. The construction is based on repeated runs of monotonic basin-hopping with L-BFGS as the local search component. We consider the standard STN to be such that a node (location) is logged as the best individual in the population every  $k$  iterations, which is the setting used in a previous STN study on population-based algorithms for continuous domains [8]. For random search, this is every  $k$  evaluations; for the other algorithms, it is every  $k \times \text{popsize}$  evaluations.

In addition to comparison with other network models, random search is included in our portfolio for validation. Random search should stall frequently and show approximately the same behaviour across all functions. That is, random search attractor networks should not look significantly different depending on the function. In addition, the attractor networks of random search should not resemble those of our other algorithms.

## 4 Experimental Setup

For our experiments, we use COCO’s [33] BBOB problem suite [34], consisting of 24 single-objective, noiseless, continuous minimisation problems, which we access via IOEXPERIMENTER [35]. We make use of a single instance (IID 1) for each problem, in both problem dimensionality 2 and 10. We consider several settings for  $\beta$ :  $\in [10, 20, 40, 80, 160, 320, 640]$  and  $\epsilon$  for the attractor networks:  $p \in [0.01, 0.001, 0.0001, 0.00001]$ . We construct attractor networks from 10 runs

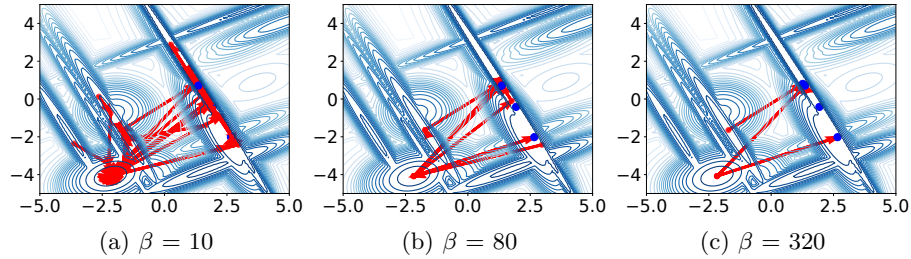


Fig. 1: Attractor networks for **CMA** on 2D Gallagher function  $f_{21}$  across different values of  $\beta$ .

and 30 runs, respectively: the smaller networks are for visualisation, while the larger ones are used for computing statistics. For both the standard LON and standard STN, we consider the same  $\epsilon$  for decision variables as the setting found in the standard LON implementation in the PFLACCO<sup>1</sup> package:  $10^{-5}$ . LON construction is implemented through PFLACCO functions and the STN construction was written from scratch in Python (the code and data will be published upon acceptance of this work). LON extraction has a parameter which serves as the termination condition for an individual run: we use the default setting for this, which is 1000 iterations without improvement. To match the attractor networks, we also construct LONs and STNs from 10 and 30 runs, for visualisation and statistics purposes, respectively. In the cases where networks relating to 10-dimensional functions are plotted, the position of nodes on the  $x$ -axis is obtained through SCIKIT-LEARN [36] multi-dimensional scaling on the decision vectors. Where search on 2-dimensional functions is visualised, the position of nodes is relative to their actual location in decision space.

Our algorithm portfolio consists of three algorithms: vanilla CMA-ES from the ModCMA package [37], DE rand/1/bin with uniform initialisation,  $F = 0.5$ ,  $Cr = 0.5$  and saturation corrections for infeasible solutions from ModDE [38] and RandomSearch taken from Nevergrad [39]<sup>2</sup>. For both modular algorithm packages, we stick with the *default parameter settings*, as we aim to illustrate the attractor network methodology rather than explore the best-performing versions of these algorithms. In particular, this decision means that the population sizes are dimensionality-dependent, with population sizes 6 and 10 for the 2 and 10-dimensional problems, respectively (which is relatively low for DE, but ensures having an equal amount of generations for both algorithms). From now on, we will refer to CMA-ES as **CMA**, DE as **DE** and random search as **RS**. In addition, the monotonic basin-hopping algorithm used in LON construction is referred to as **MBH**.

<sup>1</sup> version 1.2.2    <sup>2</sup> Versions used: modcma 1.0.2 (C++ backend), modde 0.0.1, nevergrad 1.0.0.

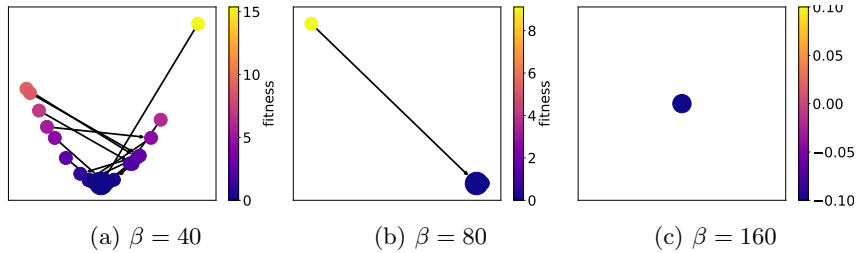


Fig. 2: Attractor networks [ $\epsilon=10^{-5}$ ] for CMA on the 10-dimensional Sphere function  $f1$  across different values of  $\beta$ . Node size is proportional to the number of runs which reached that location

## 5 Results

### 5.1 Attractor Networks: Characteristics

We begin by visualising and analysing attractor networks. Figures 1 and 2 show the change in CMA AN structure with increasing  $\beta$  (left-to-right) for  $f21$  and  $f1$ , respectively. Figure 1 reflects 2D function optimisation. The axes of the plots, and the placement of AN nodes, reflect the actual 2D coordinates; colour represents fitness. Figure 2 reflects search on 10D functions. In both Figures, we can see that increasing  $\beta$  leads to sparser attractor networks. It is interesting that for both, there are still attractors even at a high  $\beta$  — in the case of Figure 1c, which represents optimisation with a population size of 6, we can see that there are still multiple CMA attractors even with  $\beta=320$  fitness evaluations (which equates to 53 generations). Similarly, Figure 2b shows that 10-dimensional  $f1$  — the uni-modal sphere function — is associated with a sub-optimal attractor when  $\beta=80$ , which equates to 8 generations of CMA. We generated Figures for all combinations of [function, algorithm, dimension,  $\beta$ , and  $\epsilon$ ]: these can be found in the supplemental material [40].

Table 1 presents summary statistics for the distribution over the 24 functions of evaluation differentials recorded on AN edges. This reflects networks constructed with 30 runs of the algorithms and  $\epsilon=0.00001$ ; by *evaluation differential* we mean the elapsed fitness evaluations at the destination node of the edge minus the elapsed evaluations at the source node of the edge. For each network, the median differential  $md$  within it is recorded. The values in the table are the median and IQR value of  $md$  across the 24 functions is reported. Each row captures data for a given algorithm and setting for  $\beta$ . The trend is that a higher  $\beta$  leads to ANs with larger  $md$ . In the 2D case, DE has smaller  $md$  values with lower IQR value when compared to CMA. In 10 dimensions, the two have similar  $md$  values but there is a larger dispersion for DE. Random search RS has, by far, the highest  $md$  values of the three algorithms.

Figure 3 shows, for a fixed  $\beta$  setting of 320, ANs for the three considered algorithms optimising 10-dimensional Schaffer function  $f17$ . All three algorithms have ANs which look noticeably different. Random search RS has the most dense



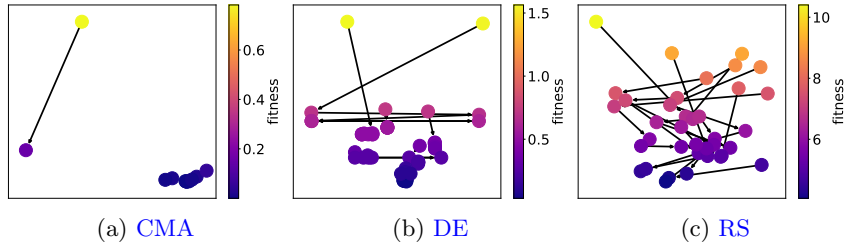


Fig. 3: Attractor networks for 10D Schaffer function  $f_{17}$ ,  $\beta = 320$ ,  $\epsilon=10^{-5}$  for different algorithms

(and most unstructured) network, and this is the trend across other functions as well (please see the supplemental material, where plots for all [function, algorithm,  $\beta$ ,  $\epsilon$ ] combinations are available [40]). The DE network is smaller and a bit more structured: by following the arrows and the horizontal spacing, we can see that as search progresses there is movement towards a particular promising region of decision space. The CMA network is smaller still; we can see that at this setting of  $\beta=320$  (that is, a stall of 32 generations), there is only a couple of sub-optimal attractors for this algorithm.

Figure 4 shows the change in network size (number of nodes) in ANs as  $\beta$  increases and for various  $\epsilon$ , for CMA (left) and random search (right) on 10-dimensional functions. For each  $\epsilon$  and  $\beta$ , there is a bar representing the median (over the 24 functions) and the variance is shown. Notice that within a coordinate precision level, nodes decrease approximately linearly with increasing  $\beta$ . In the case of CMA, a coarser  $\epsilon$  leads to more nodes, and the variance decreases substantially with  $\beta$ . For random search, low  $\beta$  leads to many fewer nodes than in the CMA counterparts, but there are still rather a lot of nodes at high  $\beta$  (the decline in network size is much less dramatic in RS than we see with CMA).

Table 1: Median and IQR value [over 24 functions] for the median evaluations differential [over all edges in a given AN with  $\epsilon=10^{-5}$  built from 30 runs]. Cells are shaded according to how often [out of 24 functions] the global optimum is present in the network: more vibrant green is more often

model	2D		10D	
	median	IQR value	median	IQR value
DE AN [ $\beta=40$ ]	52.25	6.13	55.5	67.88
DE AN [ $\beta=80$ ]	101	15.5	119.25	93.13
CMA AN [ $\beta=40$ ]	61.5	13.25	61.5	7.5
CMA AN [ $\beta=80$ ]	168	153.75	108	18.75
RS AN [ $\beta=40$ ]	509	128.63	484	126
RS AN [ $\beta=80$ ]	732.25	132.88	659.5	191.5

Figure 5 focuses on the extent to which attractor networks constructed using different configuration settings ( $\beta$  and  $\epsilon$ ) for the same functions have an overlap in the node locations for **CMA** on 2D functions. We are focussing more heavily on **CMA** than **DE**; this is because **CMA** tended to produce more interesting attractor networks. However, the same plot for **DE** can be found in the supplemental material. In Figure 5, pairs of AN configuration parameters are on each axis and the heat captures the median [across 24 functions] extent of mutual locations. For a given [vertical, horizontal] pairing, the heat value captures the fraction of the locations for the network type *on the vertical axis* which are also present in the network type *on the horizontal axis*. Squares with heat representing a value

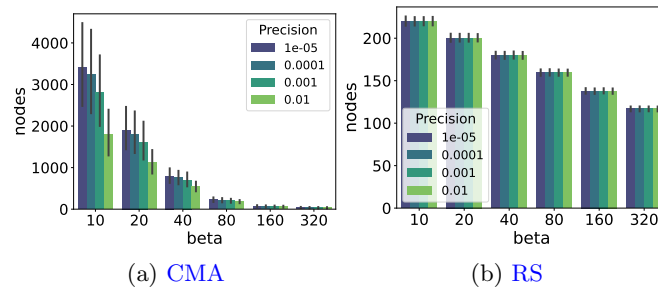


Fig. 4: 10D ANs [constructed with 30 runs] number of nodes with increasing  $\beta$  and various  $\epsilon$ .

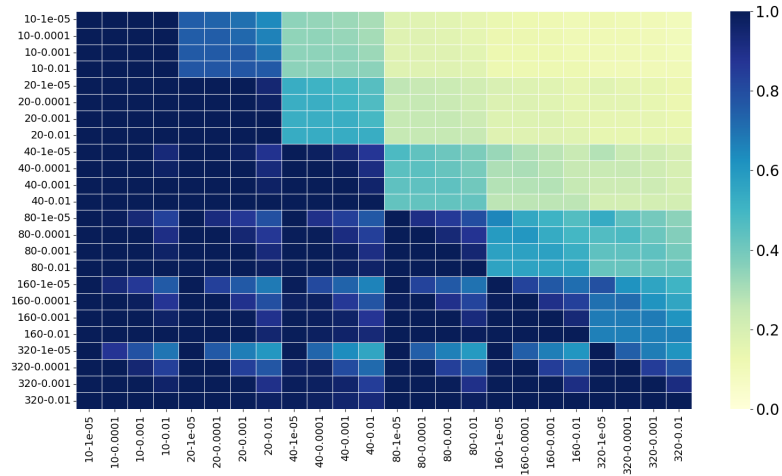


Fig. 5: The median proportion [over 24 functions] of node matches [i.e. fraction of mutual solutions] between **CMA** (2D) attractor networks with different network construction settings  $\beta$  and  $\epsilon$ . In the plot labels, the integer part is the setting for  $\beta$  and the float is for  $\epsilon$

of 1.0 indicate that across the functions, that pair of differently-configured ANs have a complete node overlap. The purpose of this plot to to further understand the properties of ANs better. Looking at the plot, we notice from the dark blue regions that ANs with the same  $\beta$  but different  $\epsilon$  are often very similar. We can also observe that networks with a different (but similar)  $\beta$  seem to frequently have some relation — although this is to a lesser extent: in the region of 40-60% of nodes matching. For the higher levels of  $\beta$  (above 80), networks are also related in this way even to network counterparts which have a substantially different  $\beta$  — for example, pairs associated with the settings 80 and 320. In the top-right of the plot, we can notice that only a low proportion of nodes present in low- $\beta$  settings are also present with high  $\beta$ , which fits with intuition.

## 5.2 Network-based Landscape Models: a Comparison

Table 1 presents the median and IQR value [over 24 functions] for network nodes and edges with respect to LONs, STNs, and ANs with different  $\beta$  configurations — all of them constructed with a  $\epsilon=10^{-5}$ . Notice that networks associated with RS are not present: this is because we noticed during STN construction that they were growing unmanageably large and deduced that they were unlikely to yield any sort of meaningful insight. Cell shading captures the proportion of the 24 functions where the associated network contains the global optimum; vibrant green means more often.

Notice from the table that DE networks have fewer nodes and edges than their CMA counterparts. Comparing the LON metrics from the first row with other network types, we can see that on 2D functions, the LONs are of similar size to DE STNs; the CMA STNs are substantially larger than both of them. In fact, the 2D CMA STNs are larger even than the 10D networks. From looking at the raw data, we see that this is because the 2D CMA STNs are often comprised of many nodes with optimal or near-optimal fitness, but which are slightly different in decision space: at least  $10^{-5}$  in one variable or more. There was a population size of six for this algorithm-dimension pair and the frequency of STN logging was every  $k$  generations, so there could be a maximum of 37500 (1250 per run for 30 runs) STN nodes if no node was ever seen twice. On 10-dimensional functions, we observe that low- $\beta$  CMA ANs are larger than LONs, but that high- $\beta$  ANs are smaller than LONs. Notice also that for most DE ANs, the IQR value for the nodes and edges is actually the same. Through investigation, we found that this happens when the number of nodes is exactly 30 more than the number of edges in the network; the reason for this phenomenon occurring is attributable to the 30 separate runs used to construct the networks, and takes place when each of the runs terminates in a different location.

Figure 6 is an illustrative comparison between different network model types: LONs, CMA STNs, and CMA ANs [with two  $\beta$  settings] are shown. Note that visualisations for the other problem instances are available in the supplemental material [40]. In the case of Figure 6, all plots reflect algorithms running on 10-dimensional Rastrign function  $f_3$ .

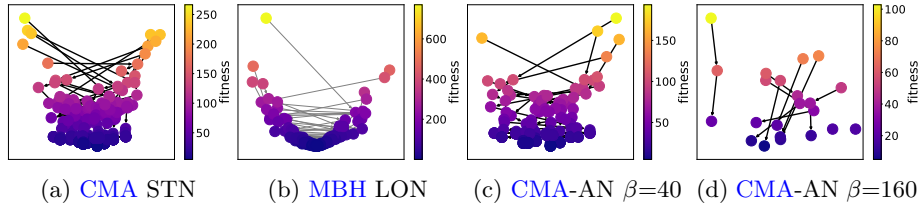


Fig. 6: Networks [ $\epsilon=10^{-5}$ ] for 10D Rosenbrock function  $f\beta$ ; the STN and AN show CMA behaviour, while the LON is constructed according to MBH (that is the convention)

Surveying the figure, we notice that the STN, the LON, and the low  $\beta$  AN seem to reveal the overall structure of how algorithms move on the problem (forming a single-funnel shape). In the case of the LON, each node had been obtained through local search. In the case of the STN (Figure 6a), nodes are not necessarily attractors. The low  $\beta$  AN resembles the STN. For the high  $\beta$  AN, there is a focus on exclusively attractors a.k.a. "local optima" for CMA. While each node in the LON (6b) is a local optimum for MBH, every node in Figure 6d is an attractor for CMA. We can see that the latter is the sparsest of the four, and allows us to see a visualisation of search trajectories with a **temporal** component than none of the other models can show: we know that CMA stalled at each of these locations for at least 160 evaluations [16 generations]. Although an STN or LON can convey how often search passed through locations, they do not convey **how long** it spent there. The STN visualised here is rather crowded and it would not be possible to know which nodes are temporal attractors. While the LON does show local optima, there are two limitations: a) the temporal aspect is not captured and b) the local optima are with respect to MBH, rather than the algorithm under study (here: CMA).

Table 2: Number of network nodes and edges for networks [ $\epsilon=10^{-5}$ ] constructed from 30 runs: median and IQR value [over 24 functions]. Cells are shaded according to how often [out of 24 functions] the global optimum is present in the network: more vibrant green is more often

model	2D		10D	
	nodes	edges	nodes	edges
LON	67.5 (143.25)	73 (164.5)	233 (521)	210 (520)
DE STN	62 (94.5)	52.5 (94.75)	86.5 (52)	77 (56.5)
CMA STN	1367.5 (2166.75)	1585 (2268.25)	559 (1320)	579 (1361.5)
DE AN [ $\beta=40$ ]	46.5 (8.25)	16.5 (8.25)	416.5 (141.25)	389 (140.25)
DE AN [ $\beta=80$ ]	31 (3)	1.5 (3)	138 (223.25)	108 (223.25)
CMA AN [ $\beta=40$ ]	104 (41.5)	96 (39.5)	860 (558.25)	830 (570)
CMA AN [ $\beta=80$ ]	44.5 (25.5)	29 (20.25)	204.5 (216.25)	196 (195.25)

The two plots in Figure 7 show the proportion of CMA AN nodes which are also present in their corresponding STN (7a) and LON (7b) respectively. The networks were constructed with 30 runs and  $\epsilon=0.01$  is used. Various  $\beta$  settings for the ANs are considered. We can observe that as  $\beta$  increases, the proportion of AN nodes increases as well. This is because there are less AN nodes and the ones which *are* still present are strong attractors; it makes sense that these nodes would also be present in the STN and LON. As  $\beta$  increases, though, the variance increases — particularly in the case of the STN matching in Figure 7a. This implies that the degree of matching as it relates to high  $\beta$  ANs may depend on the nature of the particular function. The LON overlaps are less substantial than the STN overlaps; this makes sense, because the LON is constructed using MBH, while the STNs and ANs are constructed using CMA (in this case). It seems that MBH and for CMA traverse many *different* parts of the search space and for CMA attractors do *not* seem to be equivalent to LON local optima in most cases.

## 6 Limitations and Outlook

While attractor networks (ANs) offer an interesting way for understanding algorithmic stalling behaviour across different optimization landscapes, several limitations should be taken into consideration. Firstly, the construction and interpretation of ANs depend significantly on both the algorithm and the optimisation problem. The AN assumes a single population or individual traversing the search space. Methods that introduce diversity maintenance, such as niching and quality diversity algorithms, *may* result in misleading or overly complex ANs. For these approaches with multiple subpopulations, attractors might not represent stalling but rather indicate ongoing exploration within different niches. Therefore, alternative visualizations or constructions would be required to accommodate algorithms that are inherently multimodal or explicitly diversity-promoting. Another consideration is the sample dependency in AN construction.

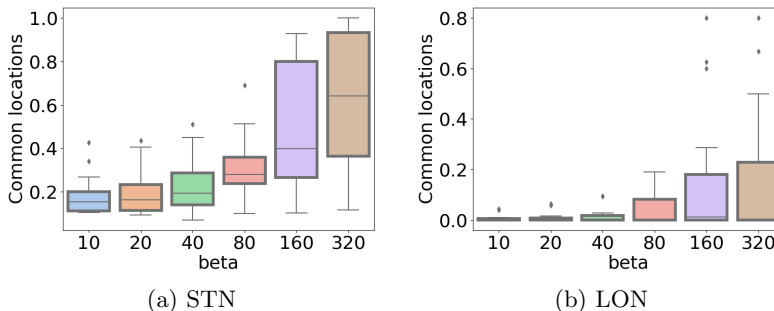


Fig. 7: CMA 10D proportion of matching locations between AN and other network models for all 24 functions [networks built with 30 runs and  $\epsilon=10^{-2}$ ] across increasing AN  $\beta$ ; represented as a proportion of AN size.

For problems with highly multimodal landscapes or higher dimensionality, the attractor network structure *may* vary substantially across different runs. This necessitates additional runs to capture a more comprehensive network structure and to ensure robustness in AN-derived insights. The use of a fixed evaluation threshold for stalling also presents limitations in long-running or fine-tuned searches, where stagnation detection would benefit from adaptive thresholds. A future direction could be to explore an increasing window for evaluation that adapts to the progression of the search. Despite these limitations, the specificity of ANs to individual algorithms also gives an advantage. It allows for algorithm-level comparisons that go beyond performance metrics alone. This could enable a more nuanced understanding of algorithm dynamics, particularly in contexts where standard metrics are insufficient to capture structural differences. Looking forward, expanding the application of ANs across diverse algorithm classes and optimization scenarios could provide a better method to analyse algorithm behaviour and problem landscapes. The AN framework can be adapted for compatibility with multimodal algorithms or for discrete problem spaces. Additionally, future studies could explore hybrid network models that integrate insights from both traditional local optima networks and search trajectory networks.

## 7 Conclusions

In this work, we formalised and put forward the notion of attractor networks (ANs) as a novel framework for analysing the stalling behaviour of optimization algorithms. By focusing on attractor points — locations in the search space where algorithms experience prolonged stagnation — ANs provide a lens for examining algorithm dynamics beyond the reach of traditional local optima networks (LONs) and search trajectory networks (STNs). Unlike LONs, which are limited to hill-climbing algorithms, and STNs, which do not typically emphasise intermediate stalling behaviour, ANs facilitate a structured view of algorithm trajectories for any optimisation approach — including those that don't use local search. Through systematic analysis across 24 BBOB functions, we demonstrated that ANs reveal meaningful contrasts in how CMA-ES, differential evolution, and random search engage with search spaces. We show that ANs can give insights into intermediate attractors where alternative network-based models of algorithm behaviour would not. The AN model's flexibility in capturing unique behavioural characteristics presents a valuable direction for comparative analysis, enabling insights into algorithm-specific stalling and convergence patterns. Future studies may adapt the AN approach to accommodate more complex multimodal search strategies, broadening the applicability of ANs within optimization research. Code and data for this paper are available in a Zenodo repository [40].

## References

1. Ochoa, G., Tomassini, M., Vérel, S., Darabos, C.: A study of nk landscapes' basins and local optima networks. In: Proceedings of the 10th annual conference on Ge-

- netic and evolutionary computation. pp. 555–562 (2008)
2. Treimun-Costa, G., Montero, E., Ochoa, G., Rojas-Morales, N.: Modelling parameter configuration spaces with local optima networks. In: Proceedings of the 2020 Genetic and Evolutionary Computation Conference. pp. 751–759 (2020)
  3. Ochoa, G., Veerapen, N., Daolio, F., Tomassini, M.: Understanding phase transitions with local optima networks: number partitioning as a case study. In: Evolutionary Computation in Combinatorial Optimization: 17th European Conference, EvoCOP 2017, Amsterdam, The Netherlands, April 19-21, 2017, Proceedings 17. pp. 233–248. Springer (2017)
  4. Ochoa, G., Chicano, F.: Local optima network analysis for max-sat. In: Proceedings of the Genetic and Evolutionary Computation Conference Companion. pp. 1430–1437 (2019)
  5. Adair, J., Ochoa, G., Malan, K.M.: Local optima networks for continuous fitness landscapes. In: Proceedings of the Genetic and Evolutionary Computation Conference Companion. pp. 1407–1414 (2019)
  6. Mitchell, P., Ochoa, G., Chassagne, R.: Local optima networks of the black box optimisation benchmark functions. In: Proceedings of the Companion Conference on Genetic and Evolutionary Computation. pp. 2072–2080 (2023)
  7. Sánchez-Díaz, X.F., Masson, C., Mengshoel, O.J.: Regularized feature selection landscapes: An empirical study of multimodality. In: International Conference on Parallel Problem Solving from Nature. pp. 409–426. Springer (2024)
  8. Ochoa, G., Malan, K.M., Blum, C.: Search trajectory networks of population-based algorithms in continuous spaces. In: International Conference on the Applications of Evolutionary Computation (Part of EvoStar). pp. 70–85. Springer (2020)
  9. Hansen, N., Auger, A., Ros, R., Mersmann, O., Tusar, T., Brockhoff, D.: COCO: a platform for comparing continuous optimizers in a black-box setting. *Optimization Methods and Software* 36(1), 114–144 (2021)
  10. Verel, S., Daolio, F., Ochoa, G., Tomassini, M.: Local optima networks with escape edges. In: Artificial Evolution: 10th International Conference, Evolution Artificielle, EA 2011, Angers, France, October 24-26, 2011, Revised Selected Papers 10. pp. 49–60. Springer (2012)
  11. Ochoa, G., Malan, K.M., Blum, C.: Search trajectory networks: A tool for analysing and visualising the behaviour of metaheuristics. *Applied Soft Computing* 109, 107492 (2021)
  12. Veerapen, N., Ochoa, G., Tinós, R., Whitley, D.: Tunnelling crossover networks for the asymmetric tsp. In: Parallel Problem Solving from Nature–PPSN XIV: 14th International Conference, Edinburgh, UK, September 17-21, 2016, Proceedings 14. pp. 994–1003. Springer (2016)
  13. Thomson, S.L., Ochoa, G.: The local optima level in chemotherapy schedule optimisation. In: European Conference on Evolutionary Computation in Combinatorial Optimization (Part of EvoStar). pp. 197–213. Springer (2020)
  14. Wright, S.J.: *Numerical optimization* (2006)
  15. Contreras-Cruz, M.A., Ochoa, G., Ramirez-Paredes, J.P.: Synthetic vs. real-world continuous landscapes: A local optima networks view. In: International Conference on Bioinspired Methods and Their Applications. pp. 3–16. Springer (2020)
  16. Karatas, M.D., Akman, O.E., Fieldsend, J.E.: Towards population-based fitness landscape analysis using local optima networks. In: Proceedings of the Genetic and Evolutionary Computation Conference Companion. pp. 1674–1682 (2021)
  17. Fieldsend, J.: Scalable local optima networks for continuous search spaces. University of Exeter (2024)

18. Homolya, V., Vinkó, T.: Leveraging local optima network properties for memetic differential evolution. In: Thi, H.A.L., Le, H.M., Dinh, T.P. (eds.) *Optimization of Complex Systems: Theory, Models, Algorithms and Applications*, pp. 109–118. Springer, Cham (2019)
19. De La Torre, C., Lavinias, Y., Cortacero, K., Luga, H., Wilson, D.G., Cussat-Blanc, S.: Multimodal adaptive graph evolution for program synthesis. In: *International Conference on Parallel Problem Solving from Nature*. pp. 306–321. Springer (2024)
20. Prager, R.P., Trautmann, H.: Pflacco: Feature-based landscape analysis of continuous and constrained optimization problems in python. *Evolutionary Computation* pp. 1–6 (2024)
21. Chacon-Sartori, C., Blum, C., Ochoa, G.: Search trajectory networks meet the web: A web application for the visual comparison of optimization algorithms. In: *Proceedings of the 2023 12th International Conference on Software and Computer Applications*. pp. 89–96 (2023)
22. Chacón Sartori, C., Blum, C., Ochoa, G.: Large language models for the automated analysis of optimization algorithms. In: *Proceedings of the Genetic and Evolutionary Computation Conference*. pp. 160–168 (2024)
23. Auger, A., Hansen, N.: A restart cma evolution strategy with increasing population size. In: *2005 IEEE Congress on Evolutionary Computation*. vol. 2, pp. 1769–1776 Vol. 2 (2005)
24. de Nobel, J., Vermetten, D., Kononova, A.V., Shir, O.M., Bäck, T.: Avoiding redundant restarts in multimodal global optimization. In: *Parallel Problem Solving from Nature – PPSN XVIII: 18th International Conference, PPSN 2024, Hagenberg, Austria, September 14–18, 2024, Proceedings, Part II*. p. 268–283. Springer-Verlag, Berlin, Heidelberg (2024)
25. Hansen, N.: Benchmarking a bi-population cma-es on the bbob-2009 function testbed. In: *Proceedings of the 11th Annual Conference Companion on Genetic and Evolutionary Computation Conference: Late Breaking Papers*. p. 2389–2396. GECCO '09, Association for Computing Machinery, New York, NY, USA (2009), <https://doi.org/10.1145/1570256.1570333>
26. Tanabe, R., Fukunaga, A.: Success-history based parameter adaptation for differential evolution. In: *Proceedings of the IEEE Congress on Evolutionary Computation (CEC)*. pp. 71–78. IEEE, Cancún, Mexico (2013)
27. Tanabe, R., Fukunaga, A.: Improving the performance of success-history based parameter adaptation for differential evolution by linear population size reduction. In: *Proceedings of the IEEE Congress on Evolutionary Computation (CEC)*. pp. 1658–1665. IEEE, Beijing, China (2014)
28. Hansen, N., Ostermeier, A.: Completely derandomized self-adaptation in evolution strategies. *Evolutionary Computation* 9(2), 159–195 (2001)
29. Kononova, A.V., Vermetten, D., Caraffini, F., Mitran, M.A., Zaharie, D.: The importance of being constrained: Dealing with constraints in evolution strategies using a new repair method. *Evolutionary Computation* 32(1), 3–25 (2024)
30. Milnor, J.: On the concept of attractor. *Communications in Mathematical Physics* 99, 177–195 (1985)
31. Collet, P., Eckmann, J.P.: *Iterated maps on the interval as dynamical systems*. Springer Science & Business Media (2009)
32. Antonov, K., Botari, T., Tukker, T., Bäck, T., van Stein, N., Kononova, A.V.: New solutions to Cooke triplet problem via analysis of attraction basins. In: Kress, B.C., Czarske, J.W. (eds.) *Digital Optical Technologies 2023*. vol. 12624, p. 126240T. International Society for Optics and Photonics, SPIE (2023), <https://doi.org/10.1117/12.2675836>



33. Hansen, N., Auger, A., Ros, R., Mersmann, O., Tušar, T., Brockhoff, D.: Coco: a platform for comparing continuous optimizers in a black-box setting. *Optimization Methods and Software* 36(1), 114–144 (2021)
34. Hansen, N., Finck, S., Ros, R., Auger, A.: Real-Parameter Black-Box Optimization Benchmarking 2009: Noiseless Functions Definitions. Research Report RR-6829, INRIA (2009), <https://hal.inria.fr/inria-00362633>
35. de Nobel, J., Ye, F., Vermetten, D., Wang, H., Doerr, C., Bäck, T.: Iohexperimenter: Benchmarking platform for iterative optimization heuristics. *Evol. Comput.* 32(3), 205–210 (2024), [https://doi.org/10.1162/evco\\_a\\_00342](https://doi.org/10.1162/evco_a_00342)
36. Pedregosa, F., Varoquaux, G., Gramfort, A., Michel, V., Thirion, B., Grisel, O., Blondel, M., Prettenhofer, P., Weiss, R., Dubourg, V., Vanderplas, J., Passos, A., Cournapeau, D., Brucher, M., Perrot, M., Duchesnay, E.: Scikit-learn: Machine learning in Python. *Journal of Machine Learning Research* 12, 2825–2830 (2011)
37. de Nobel, J., Vermetten, D., Wang, H., Doerr, C., Bäck, T.: Tuning as a means of assessing the benefits of new ideas in interplay with existing algorithmic modules. In: Krawiec, K. (ed.) *GECCO '21: Genetic and Evolutionary Computation Conference, Companion Volume*, Lille, France, July 10-14, 2021. pp. 1375–1384. ACM (2021), <https://doi.org/10.1145/3449726.3463167>
38. Vermetten, D., Caraffini, F., Kononova, A.V., Bäck, T.: Modular differential evolution. In: Silva, S., Paquete, L. (eds.) *Proceedings of the Genetic and Evolutionary Computation Conference, GECCO 2023, Lisbon, Portugal, July 15-19, 2023*. pp. 864–872. ACM (2023), <https://doi.org/10.1145/3583131.3590417>
39. Bennet, P., Doerr, C., Moreau, A., Rapin, J., Teytaud, F., Teytaud, O.: Nevergrad: black-box optimization platform. *ACM SIGEVolution* 14(1), 8–15 (2021)
40. Anonymous: Zenodo (2024), <https://zenodo.org/records/14170241>